Centrum voor Wiskunde en Informatica

Centre for Mathematics and Computer Science

P.W. Hemker, S.P. Spekreijse

Multigrid solution of the steady Euler equations

1985

Centrum voor Wiskunde en Informatica
Centre for Mathematics and Computer Science

P.W. Hemker, S.P. Spekreijse

Multigrid solution of the steady Euler equations

Multigrid Solution of the Steady Euler Equations

P.W. Hemker, S.P. Spekreijse

CWI, Centre for Mathe matics and Computer Science
P.O. Box 4079, 1009 AB Amsterdam, The Netherlands

A multigrid (MG) method for the approximation of steady solutions to the full 2-D Euler equations is described. The space discretization is obtained by the finite volume technique and Osher's approximate Riemann-solver. Symmetric Gauss-Seidel relaxation is applied to solve the nonlinear discrete system of equations. A multigrid method, the full approximation scheme, accelerates this iterative process.

In a few two-dimensional testproblems, (subsonic, transsonic and supersonic) the multigrid iteration is applied to an initial estimate that was obtained by means of the FMG-technique (nested iteration). For the discretization on the different levels, a fully consistent sequence of nested discretizations is used. The prolongations and restrictions selected are in agreement with this consistency.

It turns out that the total amount of work required to obtain a solution, that is accurate upto truncation error, corresponds to a small number of nonlinear Gauss-Seidel iterations. In the case of transsonic flow the rate of convergence of the MG-iteration appears independent of N, i.e. the number of cells in the discretization.

1980 Mathematics subject classification: 65N05, 65N30, 76G15.

1. INTRODUCTION

The Euler equations for compressible inviscid flow in a two dimensional domain Ω,

$$q_t + f_x(q) + g_y(q) = 0, \tag{1.1}$$

form a quasi-linear hyperbolic system of conservation laws. The state of the fluid at a point $(x,y) \in \Omega$ is given by $q(x,y) = (\rho, \rho u, \rho v, E)^T$. The fluxes in the $x -$ (resp. $y -$) direction are

$$f(q) = (\rho u, \rho u^2 + p, \rho uv, u(E + p))^T$$

and

$$g(q) = (\rho v, \rho vu, \rho v^2 + p, v(E + p))^T.$$

For a perfect gas, p and E are related by the equation of state

$$p = (\gamma - 1)(E - \tfrac{1}{2}\rho(u^2 + v^2)).$$

With (n_1, n_2) a pair of direction cosines, the flux in the (n_1, n_2)- direction is given by $n_1 f + n_2 g$. It is easily verified that the Euler equations are invariant under rotation of the independent variables. This means that, with the change of variables

$$\begin{bmatrix} x' \\ y' \end{bmatrix} = \begin{bmatrix} n_1 & n_2 \\ -n_2 & n_1 \end{bmatrix} \begin{bmatrix} x \\ y \end{bmatrix}$$

we obtain

$$q'_t + f_x(q') + g_y(q') = 0,$$

where

$$q' = \begin{bmatrix} 1 & 0 & 0 & 0 \\ 0 & n_1 & n_2 & 0 \\ 0 & -n_2 & n_1 & 0 \\ 0 & 0 & 0 & 1 \end{bmatrix} q.$$

Solutions of (1.1) are not necessarily smooth functions and it makes sense to generalize (1.1) to its weak form:

$$\frac{d}{dt} \iint\limits_{\Omega'} q(x,y)dxdy + \oint\limits_{\partial\Omega'} (n_1 f + n_2 g)ds = 0 , \tag{1.2}$$

for all $\Omega' \subset \Omega$.

where (n_1, n_2) is the direction of the outward normal along $\delta\Omega'$. Equation (1.2) allows also non-physical solutions and it can be shown that a physical solution should also satisfy an entropy condition [6,14].

In symbolic form we write (1.1) or (1.2) as

$$q_t + N(q) = 0. \tag{1.3}$$

The steady Euler equations are given by

$$N(q) = 0. \tag{1.4}$$

Here $N: X \to Y$ is a nonlinear operator, $X \subset [L^2(\Omega)]^4$ is the space of possible fluid states and $Y = [L^2(\Omega)]^4$ is the Banach space of rates of change (of state).

NOTATION

$\Omega \subset \mathbf{R}^2$ the domain of definition for the Euler equations.

Ω_{ij} a cell in the partitioning of Ω.

$\partial\Omega_{ij}$ the boundary of Ω_{ij}.

Ω_{ijk} a neighbouring cell of Ω_{ij}, k=N,S,E,W.

$\Gamma_{ijk} = \bar{\Omega}_{ij} \cap \bar{\Omega}_{ijk}$.

q_{ij} an approximation for the mean state in Ω_{ij}

$$q_{ij} \cdot \text{meas}\ (\Omega_{ij}) = \int\limits_{\Omega_{ij}} q(x,y)dxdy.$$

q_{ijk} an approximation for the mean state in Ω_{ijk}.

$q_h = \{q_{ij} \mid \Omega_{ij} \subset \Omega\}$.

p	pressure.
ρ	density.
u,v	speed of fluid in x,y direction.
E	total energy per unit volume.
c	$= \sqrt{\gamma p / \rho}$ speed of sound.
z	$= \ln(p\rho^{-\gamma})$ specific entropy.
γ	ratio of specific heats, $\gamma = 1.4$.

2. DISCRETIZATION

In order to achieve a discretization of a hyperbolic system of conservation laws that has a significant meaning even if the meshsize is coarse, it is important to use a fully conservative method which discretizes the weak form of the equations. A simple but effective technique is found in the finite volume discretization. This technique allows for an irregular partitioning of the domain Ω in a number of disjunct cells. For ease of notation and implementation, we divide the bounded domain Ω in quadrilateral cells Ω_{ij}, such that the result is topological equivalent with a partitioning in regular

squares. In each cell the state of the fluid is represented by q_{ij}, the mean value of $q(x,y)$ over Ω_{ij}. The semi-discrete form of the space-discretized equation is

$$\text{meas}\ (\Omega_{ij})\frac{d}{dt}\ q_{ij}\ +\ \oint_{\delta\Omega_{ij}}\ (n_1f\ +\ n_2g)ds\ =\ 0,\ \text{for all}\ \Omega_{ij}\subset\Omega, \tag{2.1}$$

where $n_1f\ +\ n_2g$ denotes the normal flux outward Ω_{ij}. For the steady equation on our mesh this reduces to

$$\sum_{k=N,E,S,W}\ \int_{\Gamma_{ij}}(n_1f\ +\ n_2g)ds\ =\ 0,\ \text{for all}\ i,j, \tag{2.2}$$

Here $\int_{\Gamma_{ij}}(n_1f\ +\ n_2g)ds$ denotes the rate of transport of q over the boundary Γ_{ijk} from cell Ω_{ij} to the neighbouring cell Ω_{ijk}, i.e. the flux from Ω_{ij} to Ω_{ijk} multiplied by meas (Γ_{ijk}). In the discretization this flux $n_1f\ +\ n_2g$ is approximated by the *numerical flux* $f(q_{ij},q_{ijk})$. In a first order discretization scheme this numerical flux over Γ_{ijk} depends only on the unknown states q_{ij} and q_{ijk}. For a given choice of the numerical flux, the discrete system for the steady equations (2.2) can formally be written

$$N_h(q_h)\ =\ 0\ . \tag{2.3}$$

This is the discrete system of nonlinear equations of which the solution is required. The operator $N_h\ :\ X_h\rightarrow Y_h$ is the nonlinear discrete operator, X_h is the (finite dimensional) linear space of mean states in cells Ω_{ij}, and Y_h is the (finite dimensional) linear space representing the rate of netto transport into the cells Ω_{ij}.

To obtain a good discretization, the selection of a good numerical flux is essential. Such a flux should take into account the fact that, depending on the local characteristics, the flux at Γ_{ijk} is -in a specific way - depending on q_{ij} and q_{ijk}. E.g. in case of a supersonic flow from Ω_{ij} to Ω_{ijk} this flux depends only on q_{ij}.

One way to determine the numerical flux is to consider the flux computation at Γ_{ijk} as a locally one-dimensional problem and to solve the Riemann problem of gasdynamics: compute the flux at Γ_{ijk}, $0<t\leqslant t_0$ with at $t=0$ the initial conditions $q=q_{ij}$ in Ω_{ij} and $q=q_{ijk}$ in Ω_{ijk}. The use of this computed flux as the numerical flux in (2.3) yields the Godunov discretization. A disadvantage is the expensive solution of the Riemann problem at each cell boundary. Several less expensive approximate Riemann solvers have been proposed. These lead to various well known flux (difference) splitting methods [2,8,9,11,12,15,17,18].

Selecting a numerical flux,we should take care that it should (1) yield shocks which satisfy correct jump conditions, (2) find only physically correct shocks, i.e. shocks satisfying an entropy condition, and (3) yield nonlinear stability (a monotone nonlinear system (2.3)).

Further it is an advantage to have a differentiable function $f(q_{ij},q_{ijk})$ if a Newton-type technique is used in the solution process for (2.3).

A very good numerical flux, that satisfies these desired properties, is generated by Osher's approximate Riemann-solver [8,9]. This numerical flux is based on the Riemann-invariants which relate different states that are connected by simple waves [14]. The good qualities of this numerical flux are often considered to be offset by its relative complexity. However, we found this disadvantage improved by the use of a proper set of dependent variables,viz. u,v,c and z [3].

An additional advantage of the numerical flux computation based on Osher's approximate Riemann solver is the fact that the treatment of boundary conditions, i.e. the computation of the boundary fluxes, can be done in a way that is completely consistent with the computation of fluxes over interior cell walls. For this purpose the equations are considered quasi-one-dimensional, normal to $\delta\Omega$, and a state q_{ijB} at the boundary $\delta\Omega_{ij}\cap\delta\Omega$ can be calculated,such that q_{ijB} satisfies the boundary conditions and such that q_{ijB} and q_{ij} are connected by Riemann invariants that correspond to negative (right boundary) or positive (left boundary) eigenvalues [3].

4

It appears that in the MG-iteration such a consistent treatment of the equation and the boundary conditions makes a special relaxation treatment of the boundary superfluous. (A similar effect is seen when an elliptic equation together with its boundary conditions is consistently dicretized by the finite element method.)

3. SOLUTION METHODS AND LINEARIZATION

Globally there are three ways to solve the nonlinear system (2.3). First, one can start from the semi-discretized form (2.1) and solve the large system of ordinary differential equations

$$D_h \frac{d}{dt} q_h + N_h(q_h) = 0 \tag{3.1}$$

by some explicit time integrator; D_h is a diagonal matrix. In this way the time-dependent behaviour of the flow is followed, starting from some initial condition. Integration over a long enough time interval may make the solution of (3.1) converge to the solution of (2.3). An advantage is that intermediate values of q_h allow a physical interpretation. If (2.3) has a non-unique solution, the proper choice of an initial condition may select the solution required. Another advantage is that this method needs only evaluations of the operator $N_h(q_h)$. If the time-dependent solution is not wanted, it is a disadvantage that usually many time-steps are needed to obtain a sufficiently converged final solution q_h. Stability conditions may prevent the use of large time steps. Multigrid may provide a technique to accelerate the convergence of this time stepping [4,13].

Secondly, the equation (2.3) may be solved by some implicit time integrator, or -what is closely related- the system (2.3) or (3.1) can be solved by some global linearization. Examples are the application of a Newton-type method or the use of the SER- (Switched Evolution Relaxation) scheme as used by Mulder and Van Leer [7],

$$[D_h + \Delta t \cdot N_h'(q_h^{(n)})] (q_h^{(n+1)} - q_h^{(n)}) = -\Delta t \cdot N_h(q_h^{(n)}) . \tag{3.2}$$

In these methods large linear systems are to be solved and the construction of the Jacobian matrix

$$N_h'(q_h)$$

is required. For the solution of the linear system (e.g. in eq. 3.2), several techniques are available. Multigrid in its linear form (the Correction Scheme) [1] can be used to accelerate iterative methods for the solution of the linear systems.

In particular Newton's method will give very fast convergence, provided that a sufficiently accurate initial estimate is available (and that a singular Jacobian is avoided). If the accurate initial estimate is not available, continuation or time-stepping techniques may slacken the solution process as was the case with the explicit time integration.

Finally, the equation (2.3) may be solved directly by means of a non-linear relaxation method. If (2.3) sufficiently satisfies stability (monotonicity) conditions, simple relaxation methods may converge. Rather than a good global convergence rate, we may expect that local relaxations -such as point Gauss-Seidel methods- will be able to smooth the error. Multigrid in its nonlinear form FAS (the Full Approximation Scheme) [1] is a proper technique to accelerate the convergence of these relaxations. The nonlinear relaxation iteration with FAS seems the most direct way to solve (2.3) and it is this approach that we follow in this paper.

In a local relaxation sweep, for each Ω_{ij} one set of four equations,

$$(N_h(q_h))_{ij} = 0 , \tag{3.3}$$

is solved (approximately). For these four equations no natural ordering exists and -hence- we solve these equations simultaneously (collective relaxation). Now only the local linearization, i.e. linearizaion of (3.3) with respect to $(q_h)_{ij}$ is needed.

Besides the reduced sensitivity for accurate initial estimates [16], it is an additional advantage of nonlinear relaxation that the storage requirements are significantly less. Only 4*4-systems are solved and no global Jacobian matrix needs to be kept, whereas a global linearization requires $80*N$ real numbers to store the Jacobian; N is the number of cells in the mesh. Probably a global linearization only pays off in a final stage of the solution process for (2.3), when Newton's method guarantees quadratic convergence. For a further discussion of the choice between Newton-Multigrid or Multigrid-Newton see [5].

Independent of the type of linearization that is actually used, it is important to see the structure of the Jacobian matrix of (2.3). For the finite volume discretization, the global Jacobian matrix is assembled in a way that is similar to the assembling process for finite elements. The finite volume Jacobian is the sum of small block-2*2 cell wall matrices (for FEM: element matrices). The regular structure of the mesh used induces a block-5-diagonal structure in which each block entry itself is a 4*4 matrix. The Jacobian and the rhs are assembled simultaneously and for each cell wall, Γ_{ijk}, the entries $\pm f(q_{ij}, q_{ijk})$,

$$\pm A_{ijk}^{+} = \pm \frac{\partial}{\partial q_{ij}} f(q_{ij}, q_{ijk}) \text{ and } \pm A_{ijk}^{-} = \pm \frac{\partial}{\partial q_{ijk}} f(q_{ij}, q_{ijk})$$

are evaluated and added as a contribution to the rhs or the Jacobian matrix respectively (see figure 1). The fact that all column sums are zero, except for boundary contributions, reflects that the discretization is conservative.

A row from the Jacobian, corresponding to the cell Ω_{ij}, is now seen to be of the form

$$-A_{i-\frac{1}{2}j}^{+} \quad , -A_{i,j-\frac{1}{2}}^{+} \quad , \begin{matrix} -A_{i,j-\frac{1}{2}}^{-} + A_{i,j+\frac{1}{2}}^{+} \\ -A_{i-\frac{1}{2}j}^{-} + A_{i+\frac{1}{2}j}^{+} \end{matrix} \quad , +A_{i,j+\frac{1}{2}}^{-} \quad , +A_{i+\frac{1}{2}j}^{-} \tag{3.4}$$

This structure of the Jacobian matrix is to be exploited when relaxation methods for the system are analyzed.
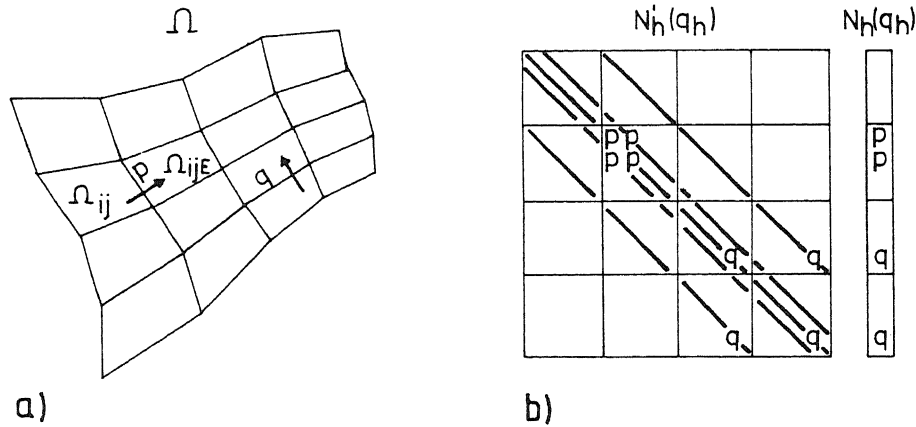

Figure 1. Assembling the rhs and the Jacobian of the nonlinear system.

In figure 1 the notation $\begin{bmatrix} P & P \\ P & P \end{bmatrix} \begin{bmatrix} P \\ P \end{bmatrix}$ is short for

$$\begin{bmatrix} +A_{ijE}^{+} & +A_{ijE}^{-} \\ -A_{ijE}^{+} & -A_{ijE}^{-} \end{bmatrix} \quad \begin{bmatrix} +f(q_{ij}, q_{ijE}) \\ -f(q_{ij}, q_{ijE}) \end{bmatrix}, \tag{3.5}$$

6

where $A_{ijE} = A_{i,j+\frac{1}{2}}$.

The boundary condition treatment is straightforward as soon as we take the view that for each $\Gamma_{ijB} = \delta\Omega \cap \bar{\Omega}_{ij}$ we can determine a q_{ijB} as is introduced in section 2. This boundary state depends on the state in the neighbouring cell: $q_{ijB} = q_{ijB}(q_{ij})$. Hence, we have for the contribution from Γ_{ijB} to (2.3)

$$f_{ijB} := f(q_{ijB}(q_{ij}), q_{ij})$$

and

$$\frac{\partial}{\partial q_{ij}} f_{ijB} = \frac{\partial}{\partial q_{ij}} f(q_{ijB}, q_{ij}) + \frac{\partial}{\partial q_{ijB}} f(q_{ijB}, q_{ij}) \cdot \qquad (3.6)$$

$$\frac{\partial}{\partial q_{ij}} q_{ijB}(q_{ij})$$

$$= A_{ijB}^{-} + A_{ijB}^{+} \cdot \frac{\partial q_{ijB}}{\partial q_{ij}} \, .$$

This completes the description of the linearization of (2.3).

The local linearization of (3.3) gives a coefficient matrix as appears in the main diagonal of (3.4). For cells near $\delta\Omega$ these systems are augmented by boundary terms as given in (3.6).

4. THE NESTED SEQUENCE OF DISCRETIZATIONS

For the P-variant of Osher's scheme [3], when the flow field is sufficiently smooth (no shocks present), for any q_h defined on the grid $\Omega_h = \{\Omega_{ij}\}$, piecewise constant states q_{ijk}^* can be defined at the cell boundaries Γ_{ijk}, such that $f(q_{ijk}^*) = f(q_{ij}, q_{ijk})$ or, at the boundary of Ω, $q_{ijk}^* = q_{ijB}$. Under these assumptions the finite volume method can be seen as a formal weighted residual method for the discretization of $N(q) = 0$.

We can write the discrete operator N_h as a Galerkin approximation to N,

$$N_h(q_h) = R_h N(P_h q_h), \qquad (4.1)$$

where $P_h : X_h \rightarrow X$ relates to each q_h a function $P_h q_h$ on Ω, for which

$$\begin{cases} P_h q_n(s) = q_{ij} & \text{for } s \in \Omega_{ij} \\ P_h q_h(s) = q_{ijk}^* & \text{for } s \in \Gamma_{ij} \end{cases},$$

where q_{ijk}^* is such that $f(q_{ijk}^*) = f(q_{ij}, q_{ijk})$. I.e. piecewise constant functions with upwind continuity at the boundaries for characteristic information.

The restriction $\bar{R}_h : Y \rightarrow Y_h$ is defined by

$$(\bar{R}_h r)_{ij} = \int_{\Omega_{ij}} r(x,y) \, dx \, dy \, ,$$

so that, formally,

$$(\bar{R}_h N(q))_{ij} = \int_{\Omega_{ij}} f_x(q) + g_y(q) \, dx \, dy$$

$$= \oint_{\delta\Omega_{ij}} n_1 f(q) + n_2 g(q) \, ds$$

$$= \sum_k \int_{\Gamma_{ijk}} (n_1 f + n_2 g) q \, ds$$

and

$$(\bar{R}_h N(P_h q_h))_{ij} = \sum_k \int_{\Gamma_{ijk}} (n_1 f + n_2 q)(P_h q_h) \, ds \qquad (4.2)$$

$$= \sum_{k \Gamma_{ijk}} \int (n_1 f + n_2 q)(q_{ijk}^*) \, ds$$

$$= \sum_{k} \text{meas} \, (\Gamma_{ijk}) f(q_{ij}, q_{ijk}) \, .$$

Now, a regular sequence of nested discretizations is found in the following way. Start with a partitioning of Ω in cells $\{\Omega_{ij} \,|\, 0 < i \leqslant n_1 2^l, 0 < j \leqslant n_2 2^l\}$. This yields the finest level of discretization (level l). For each $k = l, l-1, l-2, \ldots, 1$, a coarser level of discretization $k-1$ is defined by deleting each second meshline, so that each time 4 cells in the finer mesh correspond to a single coarser cell. In this way sequences of discrete spaces

$X_h, X_{2h}, X_{4h}, \cdots$, and $Y_h, Y_{2h}, Y_{4h}, \cdots$, are obtained. With a prolongation between the discrete solution spaces $P_{h,2h} : X_{2h} \to X_h$, defined by "piecewise constant interpolation" (distribute a coarse cell value q_{ij} as the same value over 4 finer cells), and a restriction $\overline{R}_{2h,h} : Y_h \to Y_{2h}$, defined by adding the 4 fine cell values to obtain the coarse cell value, we have the relation

$$P_{2h} = P_h P_{h,2h} \quad \text{and} \quad \overline{R}_{2h} = \overline{R}_{2h,h} \overline{R}_h \, .$$

In this way we obtain a commutative diagram for the -now nested- set of discretizations N_h, N_{2h}, etc..
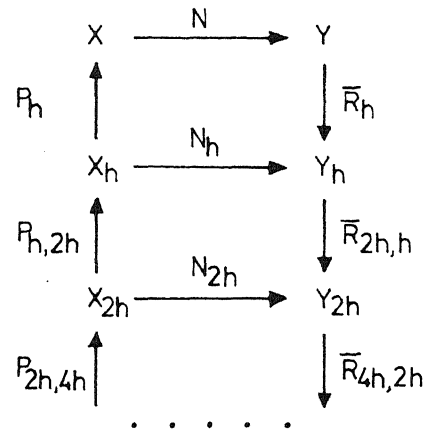

Figure 2. The nested set of discretizations.

The prolongation and restriction introduced in this way are the natural operators that correspond with the physical meanings of X and Y. An $q_h \in X_h$ is associated with the mean states of the fluid in the cells $\{\Omega_{ij}\}$, whereas $r_h \in Y_h$ is associated with the netto transport rate of the conservative quantities into the cells $\{\Omega_{ij}\}$.
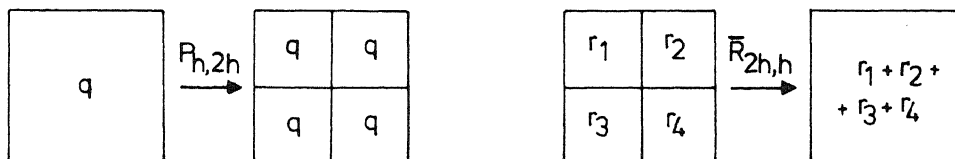

Figure 3. The first order finite volume prolongation $P_{h,2h}$ and $\overline{R}_{2h,h}$ restriction.

The operators $P_{h,2h}$ and $\bar{R}_{2h,h}$ are also used in section 5 as grid transfer operators in the FAS multigrid algorithm. In the case of CS-multigrid they can be used for the efficient construction of the coarse grid Jacobian matrices. Then the operator $\bar{R}_{2h,h} \, N_h'(q_h) P_{h,2h}$ can be used instead of $N_{2h}'(q_{2h})$. This Galerkin coarse grid Jacobian has the usual (additional) advantage that -after a coarse grid correction- the restriction of the residual vanishes and -thus- the residual contains mainly Fourier components with high frequencies.

5. THE MULTIGRID METHOD

Based on the sequence of discreizations $N_h, N_{2h}, N_{4h}, \ldots$ the Full Approximation Scheme (FAS) multigrid algorithm has been used to accelerate the nonlinear point Gauss Seidel relaxation.

One iteration step of the FAS-algorithm for the solution of $N_h(q_h) = r_h$ is defined as
1. Execution of p pre-relaxation steps.
2. Execution of a course grid correction,i.e.
   2a.   for some given q_{2h} compute

   $$r_{2h} = N_{2h}(q_{2h}) + \bar{R}_{2h,h} \, (r_h - N_h(q_h));$$

   2b.   determine by σ FAS-iteration steps $\tilde{q}_{2h}$, the approximate solution of

   $$N_{2h}(q_{2h}) = r_{2h};$$

   2c.   replace q_h by $q_h + P_{h,2h} \, (\tilde{q}_{2h} - q_{2h});$
3. execution of q post-relaxation sweeps.
On the coarsest grid no coarse grid correction is executed.

Experiments show that $\sigma > 1$ generally gives no more efficient results than $\sigma = 1$ (the V-cycle). A strategy that usually yields efficient results is $p = q = \sigma = 1$, where collective symmetric Gauss-Seidel was used as a relaxation method. The ordering of the lexicographical Gauss-Seidel relaxation was from north-west to south-east -vice versa- in the pre-relaxation, and from north-east to south-west -vice versa- during post-relaxation. This stategy was adopted as a standard strategy and it is compared with various other variants in section 6.

Initial estimates are obtained by the Full Multi Grid (FMG) technique. For $k = 0,1,2 \ldots l - 1$ the initial approximation on level $k + 1$ is obtained by
1. Application of a single FAS-cycle to the solution on level k, and
2. Interpolation of the approximate solution on level k to level $k + 1$.
For this interpolation *not* the prolongation $P_{h,2h}$ is used. The piecewise constant prolongation is not sufficiently accurate to interpolate the -first order accurate- coarse grid solution to the finer mesh. For the interpolation operator, a bilinear blockwise interpolation is used: the bilinear interpolation of the solution found on a coarse 2*2 block of cells Ω_{ij} is transfered to a 4*4 block of cells on the finer grid.

6. NUMERICAL RESULTS

To show some properties of our method, we computed flows through a channel with a circular bump. As a first test, a standard testproblem [10] was chosen. This problem concerns a transsonic flow. Further tests were made by variation of parameters, such that the flow became supersonic or subsonic. Tests were made both on adapted grids as described in [10] and on non-adapted regular square grids. In this paper, concerned with the convergence of the method rather than with the representation of the solution, we restrict ourselves to regular grids. For tests on the adapted grids the reader is refered to [3].

In a sense, the tests on a regular grid are harder because it is less clear that the coarse grid discretizations have a significant meaning for the problems on the finer grids. In particular, on the

coarsest level the meshsize was so large that the discretization cannot recognize the circular bump(!). The problem desription is given in figure 4.
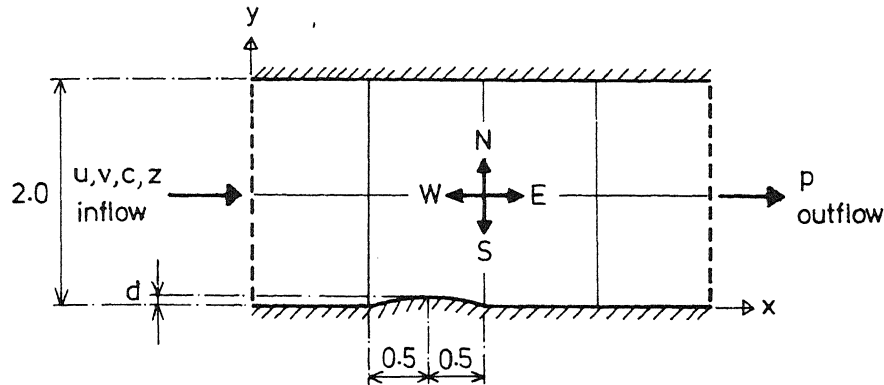

Figure 4 The testproblems

On the northern wall $v = 0$ is specified, on the southern wall the ratio v / u is specified in such a way that it is in agreement with the direction of the wall (dependent on x). At the inflow boundary u, v, z are specified. For supersonic flow on this boundary also c is given. For transonic or subsonic flow the pressure p is given at the outflow boundary. The thickness of the bump is $d = 0.042$.

The coarsest grid is a 4*2 grid, as indicated in figure 4. Finer grids were obtained by regular subdivision of the coarse cells. The boundary condition at the bump was satisfied at the mid-cell-wall. As a consequence, on the coarsest grid the boundary condition used for the southern wall is $v / u = 0$. Hence, on the coarsest grid a uniform flow is the solution of the discrete problem!

In the figures 5 to 12 we show the convergence histories of the FAS iteration for the following testproblems.

Problem 1   Supersonic flow: $u = 3.0$, $v = 0.0$, $c = 1.0$, $z = -\gamma \ln(\gamma)$
Problem 2   Transsonic flow: $u = 0.85$, $v = 0.0$, $z = \ln(p\gamma^{-\gamma})$, $p = 1.05$.
Problem 3   Subsonic flow: $u = 0.3$, $v = 0.0$, $z = \ln(p\gamma^{-\gamma})$, $p = 1.05$.

In the figures the norm of the residual, $\|N(q_h)\|$, is plotted against the iteration number. The norm used is the maximum of the four L_1-norms of the components in the residual. The numbers 2,3,4 or 5 in the figures denote the number of levels used.

The P-variant of Osher's approximate Riemann solver [3] was used for the discretization. The three problems have been run for the (standard) strategy, as described in section 5. Further experiments have run with Red-Black Gauss-Seidel relaxation. Other experiments have run with the W-cycle instead of the V-cycle.

From the experiments we conclude that for the supersonic and transsonic flow the rate of convergence of FAS is -in practice- independent of the meshwidth. Convergence is slower and dependent of the meshwith for small Machnumbers. Red-black Gauss Seidel relaxation is slower than Symmetric Gauss Seidel relaxation, but for vector architectures it may still be competitive.

If boundary conditions are over-specified, i.e. if complete states of flow are specified at the inflow and outflow boundaries (and, hence, the upwind scheme may select the best defined boundary conditions), the problem -being better posed- converges faster, as long as the number of meshpoints is small enough.

Experiments for which no figures are given, show that W-cycles give almost the same convergence behaviour as V-cycles. Bilinear prolongations in FAS give almost the same convergence behaviour as

piecewise constant prolongations. Also, when the O-variant of Osher's scheme was used [3], no significant differences were observed.

7. CONCLUSION

An efficient multigrid method for the solution of the steady Euler equations could be developed. The backbone of the method is a nested sequence of Galerkin discretizations, which is constructed by the finite volume technique. To obtain a stable discretization and a good representation of the solution (sharp captured shocks, no sonic glitches, etc.) and to find a boundary condition treatment that is consistent with the interior discretization, the use of an powerful numerical flux is essential. Such a numerical flux was found in Osher's approximate Riemann-solver.
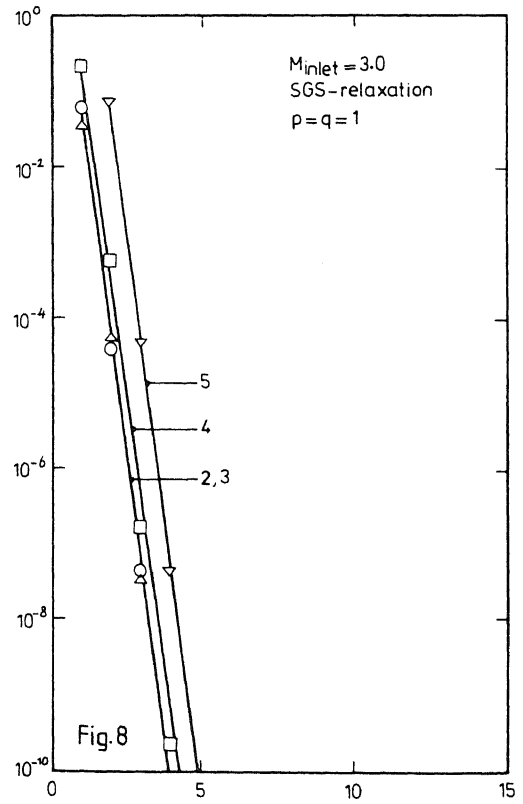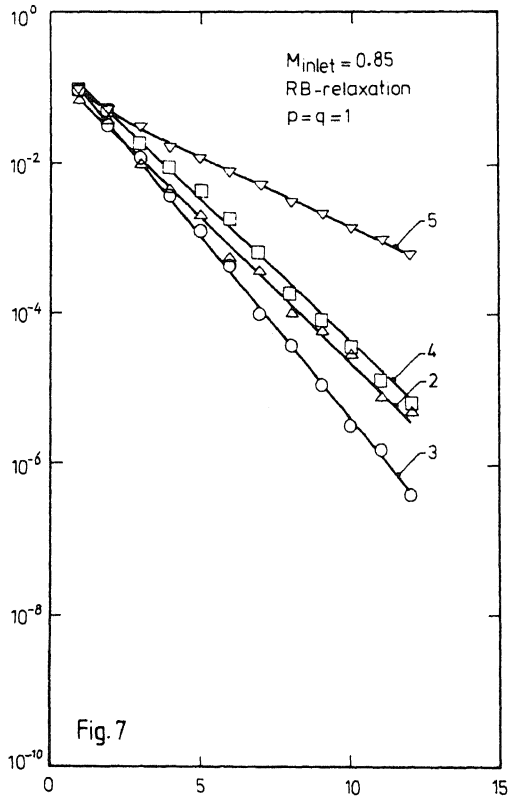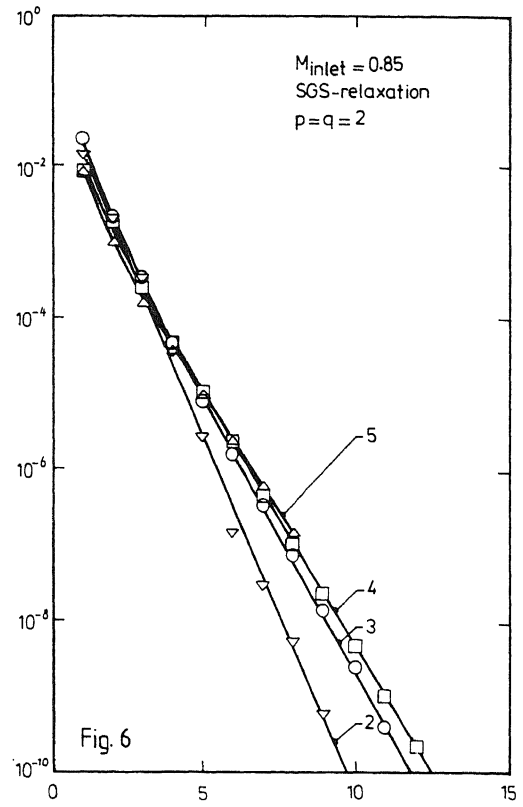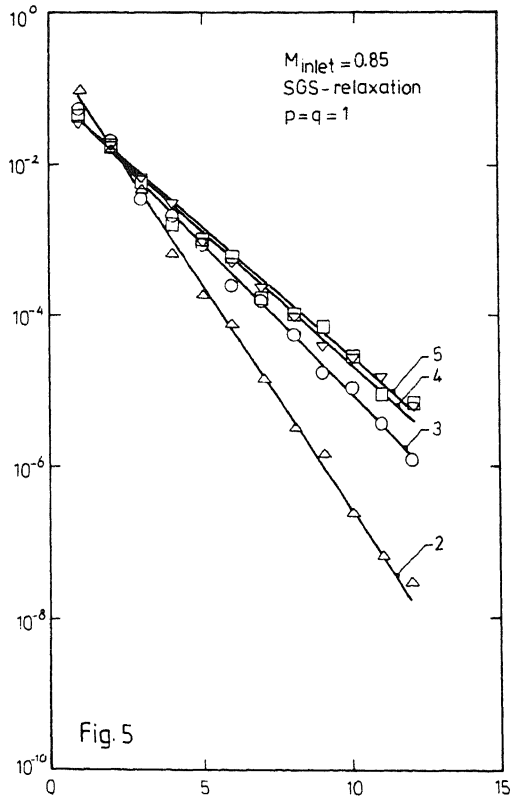
When the FMG-technique is used for the computation of initial estimates, it appears that a few FAS cycles are often enough to obtain a solution of the discrete system that is accurate upto truncation error.

Numerical experiments show that in several transsonic testcases the rate of convergence of the FAS iteration is independent of the gridsize. For a subsonic testcase, $M = 0.3$, this could not be observed.
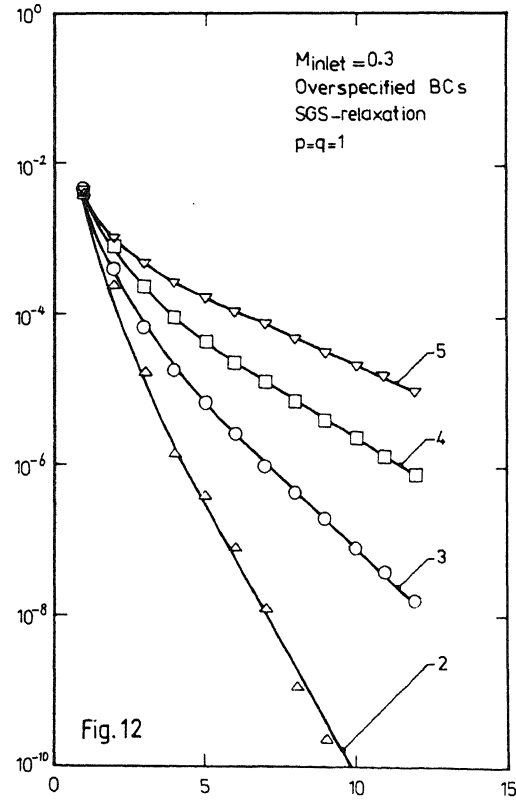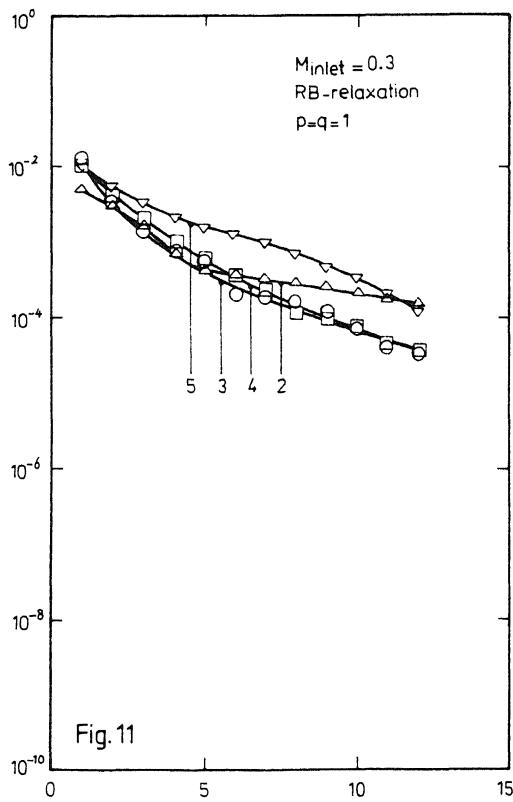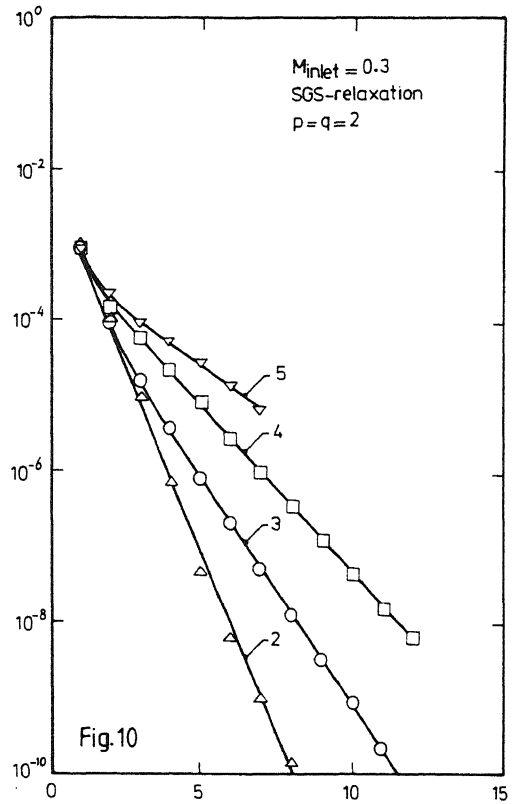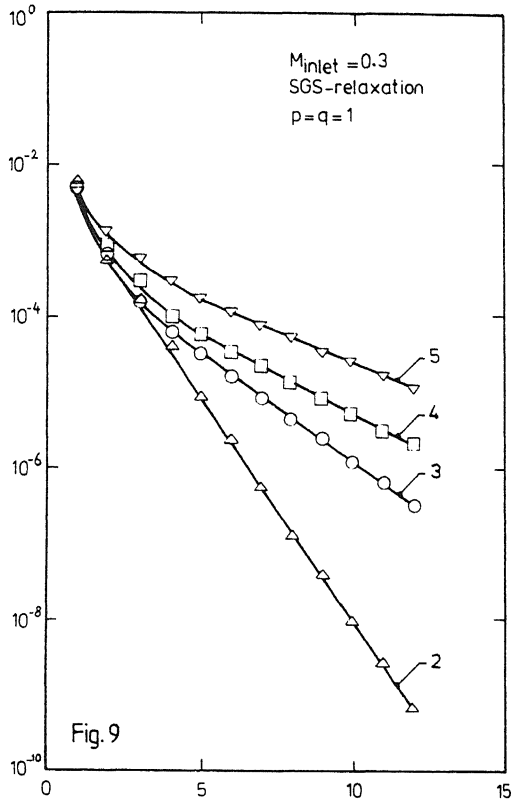
REFERENCES

[1] BRANDT, A., "Guide to Multigrid Development." In: Multigrid Methods (W. Hackbusch and U. Trottenberg eds) Lect. Notes in Mathematics 960, pp. 220-312, Springer Verlag 1982.

[2] HARTEN, A., LAX, P.D. & van LEER, B., "On upstream differencing and Godunov-type schemes for hyperbolic conservation laws." SIAM Review 25 (1983) 35-61.

[3] HEMKER, P.W. & SPEKREIJSE, S.P., "Multiple Grid and Osher's Scheme for the Efficient Solution of the Steady Euler Equations". In preparation.

[4] JAMESON, A., "Numerical Solution of the Euler Equations for Compressible Inviscid Fluids." In: Procs 6th International Conference on Computational Methods in Applied Science and Engineering, Versailles, France, Dec. 1983.

[5] JESPERSEN, D.C, "Recent developments in multigrid methods for the steady Euler equations." Lecture Notes, March 12-16, 1984, von Karman Inst., Rhode-St.Genese, Belgium.

[6] LAX, P.D., "Hyperbolic systems of conservation laws and the mathematical theory of shock waves." Regional conference series in applied mathematics 11. SIAM Publication, (1973).

[7] MULDER, W.A. "Multigrid Relaxation for the Euler equations." To appear in: J. Comp. Phys. 1985.

[8] OSHER, S. & CHAKRAVARTHY, S., "Upwind schemes and boundary conditions with applications to Euler equations in general geometries". J. Comp. Phys. 50 (1983) 447-481.

[9] OSHER, S & SOLOMON, F., "Upwind difference schemes for hyperbolic systems of conservation laws". Math. Comp. 38 (1982) 339-374.

[10] RIZZI, A. & VIVIAND, H., (Eds) "Numerical Methods for the computation of inviscid transonic flows with shock waves." Proceedings GAMM Workshop, Stockholm, 1979, Vieweg Verlag, 1981.

[11] ROE, P.L., "Approximate Riemann solvers, parameter vectors and difference schemes." J. Comp. Phys. 43 (1981) 357-372.

[12] ROE, P.L., "The use of the Riemann problem in finite difference schemes." In: Procs. 7th Int. Conf. Num. Meth. Fl. Dyn. (1980), (Reynolds & McCormack eds.) Springer Lecture Notes in Physics 141, pp.354-359, Springer Verlag 1981.

[13] RON-HO NI, "A multiple grid scheme for solving the Euler equations." AIAA Journal 20 (1982) 1565-1571.

[14] SMOLLER, J., "Shock waves and reaction diffusion equations." Grundlehren der mathematische Wissenschaften 258, Springer Verlag, 1983.

[15] STEGER, J.L., "A preliminary study of relaxation methods for the inviscid conservative gasdynamiscs equations using flux splitting." Nasa Contractor Report 3415 (1981).

[16] van ASSELT, E.J., "On M-functions and nonlinear relaxation methods." Report NW160/NW, Math.Centr., Amsterdam, 1983.

[17] van LEER, B., "Flux-vector splitting for the Euler equations." In: Procs. 8th Intern. Conf. on numerical methods in fluid dynamics, Aachen, June, 1982. Lecture Notes in Physics 170, Springer Verlag.

[18] van LEER, B., "On the relation between the upwind-differencing schemes of Godunov, Engquist-Osher and Roe." SIAM J.N.A. 5 (1984) 1.

Fig. 5

$M_{inlet} = 0.85$
SGS - relaxation
$p = q = 1$

Fig. 6

$M_{inlet} = 0.85$
SGS - relaxation
$p = q = 2$

Fig. 7

$M_{inlet} = 0.85$
RB - relaxation
$p = q = 1$

Fig. 8

$M_{inlet} = 3.0$
SGS - relaxation
$p = q = 1$

Residual (abscissa) versus number of FAS-cycles (ordinate)

Fig. 9

$M_{inlet} = 0.3$
SGS-relaxation
$p = q = 1$

Fig. 10

$M_{inlet} = 0.3$
SGS-relaxation
$p = q = 2$

Fig. 11

$M_{inlet} = 0.3$
RB-relaxation
$p = q = 1$

Fig. 12

$M_{inlet} = 0.3$
Overspecified BCs
SGS-relaxation
$p = q = 1$

Residual (abscissa) versus number of FAS-cycles (ordinate)